



## Study of Micro-hardness of High-Speed W9Mo4Co8 Steel Plates in Pendulum Grinding by Abrasive Wheel Periphery

Yakov Iosifovich Soler\* & Van Canh Nguyen

Technology and Equipment of Mechanical Manufacture Department,  
Irkutsk National Research Technical University,  
Lermontov St., Bldg. 83, 664074, Irkutsk, Russian Federation  
\*E-mail: solera@istu.irk.ru

**Abstract.** In cutting tool assembly, grinding is the most important technological step of the finishing treatment, largely determining the workmanship. An increase of micro-hardness after grinding relative to the original one indicates the dominant role of abrasive tool force impact on the ground surface. A decrease, in contrast, evidences a significant softening under the influence of heat source. This research based on nonparametric statistics to predict the effect of wheel characteristics with abrasives 25A, 92A/25A, 34A, 5A, EKE, 5NQ, TGX, 5SG and with graininess 46 (F46), 60 (F60), 80 with different porosities (structure numbers 6-12), and the expected measures of position and dispersion on the micro-hardness of the surface of a high-speed cutting plate (HSCP) made of W9Mo4Co8 steel. It was found that grinding this HSCP by wheels 5NQ46I6VS3, 5SG46K12VXP, 5SG60K12VXP, 5SG46I12VXP, 25AF46M12V5-PO, 25AF46M12V5-PO3, 25AF46M10V5-PO, 25AF46M10V5-PO3, 25AF46K10V5-PO3, 25AF60M10V5-PO3, 25AF46L10V5-KF35, EKE46K3V, 92A/25AF46L6V20 occurred without surface softening for 50% of the details from the operating batch.

**Keywords:** *abrasive wheels; grinding; measure of position and dispersion; micro-hardness; stability of the process; statistics.*

### 1 Introduction

In cutting tool assembly, grinding is the most important technological step of the finishing treatment, largely determining the workmanship. In particular, the durability of high-speed cutting plates (HSCPs) depends on the micro-hardness of their working surface. An increase relative to the original one indicates the dominant role of abrasive tool force impact on the ground surface. A decrease, in contrast, evidences a significant softening under the influence of heat source. The first phenomenon is more common in grinding by wheels of cubic boron nitride (CBN) and the second one is more common using traditional abrasives. According to the depth of 'embedding' of the grains in the bundle, abrasive grains can be divided into three groups: cutting, pressing and non-cutting grains. The cutting grains come into contact with the HSCP first, causing plastic

deformation and the cutting of microchips is observed upon reaching the contact stresses that exceed its tensile strength. Heat is allocated predominantly by friction of the abrasive grains on the juvenile surface of the newly machined metal and the energy that is expended because of its elastic and plastic deformation. In this case, during the first two stages of the cutting grains' contact with the metal, the temperature of the ground surface may be even higher than in chip removal. Pressing grains mostly slide the machined surface, intensifying the elastic and plastic deformation and heat generation. Instantaneous heating of the HSCP surface may be 700-800 °C and with heavy grinding mode up to 1200-1500 °C, leading to local melting. In this case the heating rate reaches 5000-6000 °C/s and even up to 10000 °C/s. The thermal field of the blank is characterized by a high gradient and is concentrated in the surface layer at a depth of 0.1-0.3 mm. For a few seconds this temperature decreases since the main part of the heat withdraws into the underlying layers of cold metal. The hardness is decreased on account of burns on the HSCP surface [1-4].

High-speed steels are characterized by a high concentration of carbides of the type  $M_6C$  (based on  $Fe_3W_3C$  or  $Fe_3Mo_3C$ ),  $MC$  (based on  $VC$ ) and  $M_{23}C_6$  (based on  $Cr_{23}C_6$ ). Their grindability sharply reduces in the presence of free  $VC$  carbides in the martensite structure, which have high hardness and wear resistance. In the tempering process, the carbides of the type  $M_6C$  dissolve first. In this case the proportion of  $VC$  carbides increases even more [5]. The high content of carbides in W9Mo4Co8 HSCPs on the one hand increases the resistance of cutting tools of heat-resistant and stainless steels and alloys in their treatment, and on the other hand makes work difficult for traditional grinding abrasives. Alloying elements that form carbides affect the properties of HSCPs. Tungsten carbides in particular provide an increase of hardness, heat resistance and durability but reduce strength; this increases the cost of the steel.

Chromium enhances the hardening capacity, hardenability and homogeneity of the martensitic structure and improves steel machinability before quenching. Molybdenum replaces tungsten, decreases carbide heterogeneity, increases heat conductivity, strength and viscosity but enhances the tendency towards oxidation and sensitivity to decarburization. Cobalt increases the hardness, heat resistance, thermal conductivity and wear resistance, improves grindability, but reduces strength, viscosity and plasticity, and increases sensitivity to decarburization. Tungsten and molybdenum in the presence of chromium associates bind carbon in special carbide type  $Me_6C$ , which is hard-coagulated during the tempering process, and delay the decomposition of the martensite. Vanadium improves the heat resistance, hardness, wear resistance, reduces viscosity and greatly reduces grindability.  $VC$  vanadium carbides in the highest degree intensify wear of the grinding wheel grains, because their hardness (25-

30 GPa) exceeds the hardness of the electrocorundum (18-24 GPa) used in the grinding of HSCPs [5,6].

W9Mo4Co8 and W12V3Co10Mo3 are high-performance steels. The above analysis of the influence of alloying elements on the properties of high-speed cutting tools proves that. This requires more careful selection of abrasive wheels when grinding these steels.

This study presents two types of tools: abrasive wheels (AWs) with normal porosity of the 6<sup>th</sup> structure and highly porous wheels (HPWs) with structure numbers 10; 12. The cutting ability (CA) of the AWs was enhanced by the alloying of the aluminum oxide grains and by including new materials in their grain structure: 34A; 92A/25A, 5NQ. In the latter two cases chromium-titanium and electrocorundum (*Norton Quantum X/Vitrium* wheels) were added to traditional aluminum-oxide abrasive in equal proportions, respectively. The second group, formed by HPWs, is more promising. Along with the traditional 25A grains, new abrasive materials are present in them: sinter-corundum, monocrySTALLine alumina, etc.

Sinter-corundum *SG* was manufactured (obtained) abroad by special sol-gel technology. Its physical-mechanical properties are superior to (exceed) those of electro-corundum and are close to those of cubic boron nitride (CBN). However, *SG* grains are easier to straighten; the amount of straightening is reduced by 80% compared to electro-corundum. Their destruction occurs in the form of microparticles that are 100-500 times smaller than the grains of white-fused alumina. This provides the *SG* grains with an increased strength of up to three times and operation in self-sharpening mode by updating new cutting edges with minimal wear. This study used 5*SG* HPWs in which traditional grains of aluminum oxide were added to *SG* grains in equal proportion [7,8]. The latest development of the firm *Norton* is *TGX* grains. They have the form of threads with a ratio of length *l* to diameter *d* equal to 8. In *Altos* wheels they are present at a ratio of 1:1 with *SG* grains. *Altos* wheels have a high natural porosity and provide heavy metal removal during deep grinding [9,10]. In this work, also monocrySTALLine corundum (mark 5A and *EKE* from the company *Carborundum Abrasives*) was used, which provides easy cutting of metal.

Another promising direction for solving this problem is the use of HPWs from cubic boron nitride when high-speed grinding of high-performance steel. In [11], grinding of W9Mo4Co8 HSCPs was performed by eleven HPWs of CBN without visible burns. The greatest strengthening of the surface  $HV = 11267-11447$  MPa was ensured by the CBN30 B126 100 L V K27 – (KF 25, KF40) HPWs. They differed only in the size of poreforming: 0.25 and 0.40 mm. In none of the grinding cases, surface micro-hardness was better than the initial

7200 MPa. However, because of their high cost, the complicated dressing and profiling does not allow the CBN HPWs to take the leading positions when grinding high-speed cutting tools.

The purpose of this research was to increase grinding efficiency, which provides an increase of the micro-hardness of W9Mo4Co8 and W12V3Co10Mo3 HSCPs in pendulum grinding by the periphery of the abrasive tools.

## 2 Methodology of Experiments

The procedure is organically divided into two stages: the conditions of the natural experiment and statistical methods for interpretation of the experimental data.

### 2.1 Conditions of Natural Experiment

Experiments were carried out according to the scheme of the pendulum removal operating allowance when grinding by the periphery of AWs and HPWs. The following conditions of experiment realization were held constant: plane-grinding machine of model 3G71; cutting mode – cutting speed  $v_w = 35$  m/s; longitudinal feed  $S_l = 7$  m/min; cross-feed  $S_c = 1$  mm/double stroke; cutting depth  $t = 0.015$  mm; operational allowance  $z = 0.15$  mm; coolant – 5% emulsion Akvol-6 (Technical Specifications TU 0258-00148843-98) fed on detail with the consumption of 7-10 l/min; wheel conditioning operation was fulfilled before every test by synthetic diamond pencil 3908-0088 (Technical Specifications TU 2-037-0221933-001089, type 02), which was installed in a fixture on the magnetic plate of the machine in the mode: cross feed  $S_c = 1-2$  mm/double stroke, cutting depth  $t = 0.005-0.01$  mm; the number of wheel conditioning operations was 4-6; the research object was an HSCPs made of W9Mo4Co8 steel (66-68 HRC) with the following dimensions: diameter  $D = 40$  mm, height  $H = 40$  mm, which was mounted on the magnetic plate of the machine, its initial micro-hardness  $HV_{in} = 7201$  MPa; the number of parallel experiments  $n = 30$  ( $v = \overline{1;30}$ ); shape and size of the circles were 1 (01) 250 x 20 x 76 mm, which in both cases correspond to the direct profile: ‘1’ according to GOST (Russian State Standard Specification) P 52731-2007 and the catalogue of the *Carborundum Abrasives* company; ‘01’ according to the catalogue of the *Norton* company.

In general terms, the output variables of the grinding process are presented in the form:  $\{y_{iv}\}$ ,  $i = \overline{1;16}$ , where the index  $i$  carries in a compressed form information about the characteristics of the used wheels: 1 – 5NQ46I6VS3, 2 – 5SG46K12VXP, 3 – 5SG60K12VXP, 4 – 5SG46I12VXP, 5 – TGX80I12VCF5,

6 – 25AF46M12V5–ΠO, 7 – 25AF46M12V5–PO3, 8 – 25AF46M10V5–PO, 9 – 25AF46M10V5–PO3, 10 – 25AF46K10V5–PO3, 11 – 25AF60M10V5–PO, 12 – 25AF46L10V5–KF35, 13 – 5A46L10VAX, 14 – EKE46K3V, 15 – 92A/25AF46L6V20, 16 – 34AF60K6V5. Graininess of wheels of Russian origin (GOST P 52381-2005) corresponds to (matches with) ISO 8486-1:1996. They have the letter F added in order not to confuse them with grain size according to GOST 3647-80.

Wheel hardness designations according to GOST P 52587-2006 and ISO 525:1999 are the same. AW Norton Vitrium  $i = 1$  was chosen as the basic tool. The  $i = 13; 14$  wheels were made by *Dorfner Schleifmittelwerk* (Germany). The monocrystalline alumina designation in these wheels depends on the method of tool manufacture: ‘EKE’ for cast wheels and ‘5A’ for pressed wheels. The marking of other elements of the wheel ( $i = 14$ ) characteristics corresponds largely to the Russian and Norton catalogues, except for the structure numbers: in  $i = 2; 12$  structure wheels 10-12 refer to highly porous, and for the  $i = 13$  wheel, the 10<sup>th</sup> structure is considered open porosity, and the structures of the 13-20 wheels as highly porous. In the cast tool, the index ‘K’ indicates the average structure, and number 3 a ‘soft’ hardness.

The micro-hardness,  $HV$ , was measured on the PMT-3 device according to the method as described in [12] under the following conditions: the load is  $P = 1.96$  N (200 gf), the lowering speed of the indenter is 0.15 mm/s, the holding time under load  $10 \div 15$  s. The measurements  $HV_{id}$  were carried out at three points  $d = \overline{1;3}$  (Figure 1).

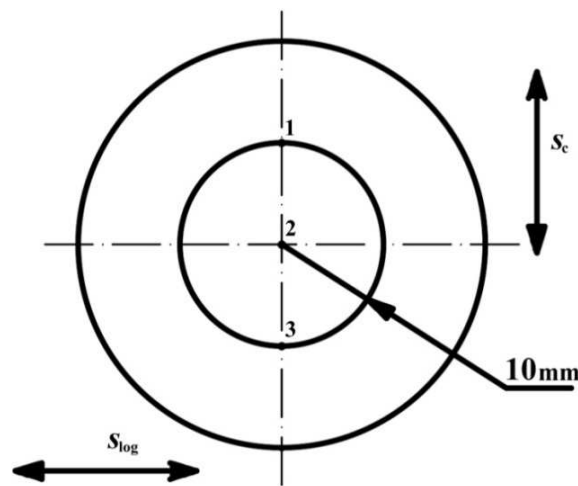


**Figure 1** Scheme of HSCP surface micro-hardness measurement.

The micro-hardness, measured in points  $d = \overline{1;3}$ , reflects the conditions of cold work hardening formation on spark-out pass when the HSCP is moved along vector  $s_c$  to the operator:  $d = 3$  for wheel penetration into the HSCP in conditions of non-stationary cutting;  $d = 2$  for stationary cutting in conditions of constant contact between the HSCP and the wheel;  $d = 1$  for non-stationary cutting conditions when the HSCP exits contact with the wheel. As will be shown below, the micro-hardness at these points did not differ significantly. In this regard, the estimated overall average and the degree of cold work hardening is found from the expression in Eq. (1):

$$\Delta HV_i = \left[ \left( \overline{HV}_i - HV_{in} \right) / HV_{in} \right] \cdot 100\% \quad (1)$$

## 2.2 Statistical Methods for Interpretation of Experimental Data

Thermal physics and dynamics of the grinding process are characterized by significant instability, which is conditioned by the location of undirected grains in the wheel's crotch, the large dispersion of the tool edge radius and the different angles in the height of the tips of the cutting edge tools. This fact allows us to consider the cutting ability of wheels as random values (RV) and for interpretation of experimental data it is advisable to use probability-theoretic methods. In view of the foregoing, the experimental data are analyzed:

$$\{y_{iv}\}, \quad i = \overline{1;16}, \quad v = \overline{1;30}, \quad (2)$$

using parametric and nonparametric (rank-based method) statistical methods. The characteristics of one-dimensional frequency distribution for Eq. (2) are [13-15]: for the first direction, averages  $\bar{y}_i = y_{i\bullet}$ , standard deviations  $SD_i$  and swing  $R_i = (y_{\max} - y_{\min})_i$ ; for the second direction, medians  $\tilde{y}_i$  and quartile width  $QW_i = (y_{0.75} - y_{0.25})_i$ . In both cases, the 1<sup>st</sup> frequency characterizes the measure of position (reference value) and subsequent frequencies characterize the measure of dispersion (precision).

Each statistical method has specific applications at which it is effective [13] for use in technical applications. It is necessary for the parametric method that the observations in Eq. (2) have the properties of homoscedasticity (synonyms – uniformity or homogeneity) of deviation variances  $(SD)_i^2$ ,  $i = \overline{1;16}$  and normality of distributions. Otherwise, the exact criteria of this method lose their reliability and can lead to incorrect statistical decisions. In this situation it is better to use rank statistics that are not associated with any family of distributions and do not use their properties. The choice of statistical method and the subsequent search of the expected averages  $\hat{y}_{i\bullet}$  and medians  $m\hat{y}_i$ ,

$i = \overline{1;16}$  are presented in [14]. This study was confined to the statement of the fact that the interpretation procedure of Eq. (2) includes two sequentially executed stages. Initially, unidimensional variance analysis (UVA) is performed to identify significant differences between the levels of the measures of position without their roll-call search. This procedure is completed in a second stage by establishing predictable averages  $\hat{y}_{i\bullet}$  and medians  $m\hat{y}_i$ ,  $i = \overline{1;16}$ .

The influence of the nonparametric method on the reference value is represented by the median coefficients of the same name,  $i = \overline{1;16}$ :

$$K_{Mi} = \tilde{y}_i / y_{i\bullet} \quad (3)$$

Evaluation of wheel CA relative to the base AW 5NQ46I6VS3 ( $i = 1$ ) was carried out for both characteristics of the univariate frequency distribution of Eq. (2) [13,14,16]:

$$K_i = \tilde{y}_i / \tilde{y}_1, \quad (4)$$

$$\hat{K}_i = m\hat{y}_i / m\hat{y}_1, \quad (5)$$

$$K_{Sti1} = SD_1 / SD_i, \quad (6)$$

$$K_{Sti2} = R_1 / R_i, \quad (7)$$

$$K_{Sti3} = QW_1 / QW_i, \quad (8)$$

where the indexes  $j = \overline{1;3}$  in the grinding stabilizing coefficients of Eqs. (6)-(8) reflect the adopted measures of dispersion: 1 –  $SD_i$  Eq. (6); 2 –  $R_i$  Eq. (7) for parametric statistics; 3 –  $QW_i$  Eq. (8) for rank statistics.

Coefficients of stability were obtained by mapping the index of reproducibility [16]:  $K_{Stj} = C_{pjalter} / C_{pjbasic}$ , where  $C_{pjalter}$ ,  $C_{pjbasic}$  are the alternative and the basic options of grinding for the actual spreads (2) without taking into account the tolerance of their scattering with the same name,  $j = \overline{1;3}$ .

### 3 Research Results and Discussion

#### 3.1 Justification of Statistical Method for Interpretation of Experimental Data

Testing Eq. (2) for homogeneity of variance [14,17] revealed that the requirement of the parametric statistics method was violated comprehensively. The second requirement, for normality of distributions, is less strict because parametric methods are robust to moderate violations of normality of distributions Eq. (2). This requirement was partially violated. The null-hypothesis was accepted for 4 wheels out of 16, namely  $i = 3; 9; 14; 16$ . In view of this situation, the main focus of the study was moved to a univariate frequency distribution of rank statistics: medians and quartile width. Parallel measures of position and dispersion of the parametric method played a supporting role, primarily destined to identify the danger of their use 'in a foreign field'.

#### 3.2 Microhardness and Degree of Cold Hardening of W9Mo4Co8 HSCPs in Areas of Grinding

The results of micro-hardness measurement and calculating of cold hardening degree according to Eq. (1) were obtained by grinding W9Mo4Co8 HSCPs by wheels  $i = \overline{1;16}$  (presented in Table 1). It was established that a single regularity of micro-hardness variation in the zones  $d = \overline{1;3}$  was absent. In this regard,  $\overline{HV}_{id}$  were submitted in the overall averages  $HV_{i..}$  and according to these resulting degrees of cold hardening  $\Delta HV_{i..}$  were calculated (presented in the last column of Table 1). They confirmed the results [2] obtained in similar conditions during grinding of a W12V3Co10Mo3 HSCP (last column).

**Table 1** Micro-hardness and degree of cold hardening at measurement points obtained during grinding of W9Mo4Co8 HSCPs with wheels  $i = \overline{1;16}$ .

Wheels $i$	Measurement points $d$						$\Delta HV_{i..}$ , %	$\Delta HV_{i..}^*$ , %
	1		2		3			
	$\overline{HV}_{i1}$ , MPa	$\Delta HV_{i1}$ , %	$\overline{HV}_{i2}$ , MPa	$\Delta HV_{i2}$ , %	$\overline{HV}_{i3}$ , MPa	$\Delta HV_{i3}$ , %		
1	9069.565	25.95	8880.04	23.32	8753.02	21.55	23.61	-0.54
2	7578.965	5.25	7851.00	9.03	7519.30	4.42	6.23	12.91
3	8052.276	11.82	7872.88	9.33	7951.80	10.43	10.53	-14.47
4	7964.674	10.61	7951.56	10.42	8001.64	11.12	10.72	-
5	6411.962	-10.96	6351.93	-11.79	6136.58	-14.78	-12.51	7.85
6	9818.120	36.34	9229.19	28.17	9940.11	38.04	34.18	18.49

**Table 1 Continued.** Micro-hardness and degree of cold hardening at measurement points obtained during grinding of W9Mo4Co8 HSCPs with wheels  $i = 1; 16$ .

Wheels $i$	Measurement points $d$						$\Delta HV_{i..}$ , %	$\Delta HV_{i..}^*$ , %
	1		2		3			
	$\overline{HV}_{f1}$ , MPa	$\Delta HV_{f1}$ , %	$\overline{HV}_{f2}$ , MPa	$\Delta HV_{f2}$ , %	$\overline{HV}_{f3}$ , MPa	$\Delta HV_{f3}$ , %		
7	7727.911	7.32	7656.70	6.33	7688.95	6.78	6.81	-10.96
8	9943.429	38.08	10746.04	49.23	10422.20	44.73	44.02	12.80
9	9180.438	27.49	8876.74	23.27	9027.04	25.36	25.37	-12.22
10	8445.318	17.28	8158.92	13.30	8229.28	14.28	14.95	-12.22
11	7442.440	3.35	7786.10	8.13	7573.60	5.17	5.55	6.20
12	7302.293	1.41	7833.37	8.78	7576.27	5.21	5.13	-3.14
13	5943.445	-17.46	6059.95	-15.85	6032.20	-16.23	-16.51	-5.28
14	8167.350	13.42	8383.47	16.42	8870.99	23.19	17.68	-
15	7323.225	1.70	7215.92	0.21	7485.12	3.95	1.95	22.00
16	6712.336	-6.79	6794.64	-5.64	6917.59	-3.94	-5.45	20.24

Note: the sign '-' indicates surface softening. Wheels  $i$  – see methodology of the experiment.  $\Delta HV_{i..}^*$  for W12V3Co10Mo3 HSCP [2].

Discussion of the study results proceeds from the fact that the increase of the cold hardening degree of the HSCP surface reduces its attrition wear rate during cutting. At the same time, the above indicates an increase of wheel CA. The work [19] reports that under pendulum grinding conditions, the sintercorundum HPW showed lower cutting forces in comparison with grains of electrocorundum. It was assumed that the smaller degrees  $\Delta HV_{i..}$ , for wheel  $i = 2$  (Table 1) are a consequence of less exposure to the process dynamics compared to the HWP's  $i = 8; 12$  with 25A grains. However, the study of burns ( $B_i$ , %) by the method of [18] for wheels  $i = 1; 3; 6; 8; 9$  (Table 2) pointed out that this phenomenon is due to the increase of heat source.

According to the reduction of the cold work hardening degree, the wheels' CA is characterized by a decreasing sequence: 25AF46M10V5-PO (44.02%) > 25AF46M12V5-PO (34.18%) > 25AF46M10V5-PO3 (25.37%) > 5NQ46I6VS3 (23.61%) > EKE46K3V (17.68%) > 25AF46K10V5-PO3 (14.95%) > 5SG46I12VXP (10.72%) > 5SG60K12VXP (10.53%) > 25AF46M12V5-PO3 (6.81%) > 5SG46K12VXP (6.23%) > 25AF60M10V5-PO3 (5.55%) > 25AF46L10V5-KF35 (5.13%) > 92A/25AF46L6V20 (1.95%). This lets us state that the greatest surface hardening was provided by the Russian HPW  $i = 6; 8; 9$  and the Norton Vitrium AW of normal porosity. Micro-hardness according to HPW  $I$  ranks as follows:  $14 > 10 > 4 > 3 > 7 > 2 > 11 > 12 > 15$ . Wheels ( $i = 3; 4$ ); ( $i = 2; 7$ ) and ( $i = 11; 12$ ) practically showed the same cold hardening:

(10.53-10.72%); (6.23-6.81%) and (5.13-5.55%). The other tools caused softening of the following HSCPs: 34AF60K6V5 ( $\Delta HV_{16\bullet} = -5.45\%$ ), TGX80I12VCF5 ( $\Delta HV_{5\bullet} = -12.51\%$ ) and 5A46L10VAX ( $\Delta HV_{13\bullet} = -16.51\%$ ). Additionally, the degrees of the W12V3Co10Mo3 [2] HSCP's cold hardening are shown. This steel has lower machinability by grinding compared to W9Mo4Co8. For this steel it should be noted first of all that the greatest hardening decrease of the W12V3Co10Mo3 HSCPs was 20.24-22%. This phenomenon is caused by the increase of cutting temperature.

The number of softening cases of W12V3Co10Mo3 HSCPs increased from four to seven, although the range of the tested wheels was reduced by two. There are new priorities in the evaluation of the wheels' CA. The  $i = 15; 16; 7$  wheels of Russian production performed best, providing hardening  $\Delta HV_{i\bullet} = 22 - 18.48\%$ . The 5SG46K12VXP HPW is recognized as the best of the *Norton* wheels during W12V3Co10Mo3 HSCP hardening with  $\Delta HV_{2\bullet} = 12.91\%$ . The *Altos* wheel ( $i = 5$ ), both in the case of W9Mo4Co8 and of W12V3Co10Mo3 steel grinding, did not reach its highest CA. Perhaps this is due to the fact that a pendulum scheme of allowance cutting the small depth  $t$  was assigned, while the *Altos* wheels are designed for creep feed grinding per one pass.

Let us now first focus on the role of individual elements of the wheel characteristics in the micro-hardness formation of the HSCP surface. The tool hardness of *Norton* HPW  $i = 2; 4$  of the 12<sup>th</sup> structure changed from  $K$  (medium soft grade) to  $I$  (soft), i.e. three degrees. In the grinding process of W9Mo4Co8 HSCPs the intensity of cold hardening ranged from 4.42 to 11.12%, i.e. it increased 2.5 times. As is known, at the firing temperature, the bundle has good adhesion with the abrasive grains. As a result, the individual grains are connected by so-called bridges consisting of the bundle's material. The large surface energy of the bundle contributes to the shaping of separate grains into the whole skeleton. Bundle bridges of soft grade wheels have more plasticity, reducing the tool elastic modulus in general [19]. In the grinding process, the cutting force  $P_y$  presses the most protruding grains into the bundle more easily. Additional grains may enter into the work, whereby the operating allowance is removed with a smaller thickness of cut, which is accompanied by a reduction of heat impulses and cutting temperature in general. In this case, the degree of cold hardening of the surface of the W9Mo4Co8 HSCPs increased. Similar results were obtained during grinding with monocrundum wheels  $i = 13; 14$ . In this case, a cast wheel with a 'soft' hardness during the grinding of the W9Mo4Co8 HSCPs showed surface hardening  $\Delta HV = 17.68\%$  and a pressed wheel ( $i = 13$ ) with hardness  $L$  (medium soft) showed softening

$\Delta HV = -16.51\%$ . Softening was validated on the W12V3Co10Mo3 HSCPs. The hardness of 25A HPWs characterized by the 10<sup>th</sup> structure also varied over 3 degrees: from *M* (medium) to *K*. But the hardness shifted to a more stable confinement range of grains in the wheel crotch, with less compliance. It is quite likely that in this range of hardness, the abovementioned regularities do not reveal themselves significantly: on the W9Mo4Co8 HSCPs the hardness decrease of the wheel was accompanied by a decrease in cold-hardening degree (Table 1) and the surface softening was revised on the W12V3Co10Mo3 HSCPs equally for both harnesses.

It turned out that the graininess of the HPWs correlated with the abrasive materials and the marks of the HSCPs. The smaller grains of 5SG60 in HPW  $i = 3$  better grinded the W9Mo4Co8 HSCPs and the larger grains of 5SG46 in HPW  $i = 2$  better grinded the W12V3Co10Mo3 HSCP. In HPWs  $i = 8; 11$  with grains 25AF46 and 25AF60 a higher degree of cold work hardening was revealed with graininess F46 for grinding of both steel grades.

**Table 2** Influence of wheel characteristics on reference values of microhardness, coefficients of (3)-(5) and burn marks.

Wheel $i$	$HV_i, \text{MPa} / B_i, \%$				$K_M$ (3)	$K_i$ (4)	$\hat{K}_i$ (5)
	$y_i$	$\tilde{y}_i$	$\hat{y}_i$	$m\hat{y}_i$			
1	8900.87	8895.90	8807.41	8860.43	0.999	1.000	1.000
	61.90	62.29	60.57	59.61	1.006	1.000	1.000
2	7649.75	7747.19	7716.86	7746.32	1.013	0.871	0.874
3	7958.98	7918.75	7852.00	8053.44	0.995	0.890	0.909
	63.35	61.79	61.72	60.35	0.975	0.992	1.019
4	7972.62	8033.13	7852.00	8053.44	1.008	0.903	0.909
5	6300.16	6002.68	6264.71	6797.66	0.953	0.675	0.767
6	9662.48	9445.00	9528.08	9155.25	0.977	1.062	1.033
	57.20	56.97	58.64	57.21	0.996	0.915	0.966
7	7691.18	7861.56	7716.86	7746.32	1.022	0.884	0.874
8	10370.56	10553.73	10311.55	9496.81	1.018	1.186	1.072
	48.96	49.14	50.42	53.99	1.004	0.789	0.912
9	9028.07	9092.63	8965.79	8860.43	1.007	1.022	1.000
	54.81	55.87	55.18	56.07	1.019	0.897	0.947
10	8277.84	8376.25	8125.47	8258.4	1.012	0.942	0.932
11	7600.71	7487.75	7704.48	7587.81	0.985	0.842	0.856
12	7570.64	7416.25	7673.29	7587.81	0.980	0.834	0.856
13	6011.86	5824.95	6192.24	6230.52	0.969	0.655	0.703
14	8473.93	8568.03	8351.82	8258.4	1.011	0.963	0.932
15	7341.42	7190.38	7585.50	7391.29	0.979	0.808	0.834
16	6808.19	6863.94	6863.25	7049.34	1.008	0.772	0.796

Note: 1 – wheels  $i$  (see methodology of the experiment); 2 – burn marks

Now we focus on the effectiveness of the cellululating agent: PO, PO3, KF35 in the Russian HPWs  $i = 8; 9; 12$  with the 10<sup>th</sup> structure PO and PO3 in the HPWs  $i = 6; 7$  with the 12<sup>th</sup> structure. The most well known among them is the additive KF35, where KF denotes fruit stone, while number 35 indicates the fineness of their main fraction: 0.35 mm. During burring of the wheel workpiece, fruit stones burn out with the formation of large interstices. No information about the chemical composition of fillers PO and PO3 is provided by the manufacturers because it is a commercial secret. Therefore we will confine the discussion to their practical application. It has been established that during W9Mo4Co8 HSCP grinding, the 25AF46M(L)10V5 HPWs showed the following results of hardening, taking into account the cellululating agents: PO ( $I = 8$ )– $\Delta HV = 44.02\%$ , PO3 ( $i = 9$ )– $\Delta HV = 25.37\%$ , KF35 ( $i = 12$ )– $\Delta HV = 5.13\%$ . In a similar situation, a greater surface softening took place for the W12V3Co10Mo3 HSCPs: 12.8%, (–12.22%) and (–3.14 %), respectively. The PO agent performed best for both steels. Two HPWs were tested for the 12<sup>th</sup> structure; they confirmed the superiority of cellululating agent PO over PO3.

Heat dissipation greatly decreased during the grinding of the HPWs and as a result, the temperature in the contact zone was reduced by almost 3 times [20]. Herewith, an increasing degree of cold working should be expected. 92A/25AF46L6V20 ( $i = 15$ ) was taken as a wheel with normal porosity; 25AF46M10V5-PO ( $i = 9$ ) and 25AF46M12V5-PO ( $i = 6$ ) were used as HPWs. As can be seen from Table 1, during grinding of the W9Mo4Co8 HSCPs,  $\Delta HV_{15..} = 1.95\%$  took place for the 6<sup>th</sup> structure,  $\Delta HV_{9..} = 25.37\%$  for the 10<sup>th</sup> structure and  $\Delta HV_{6..} = 34.18\%$  for the 12<sup>th</sup> structure. The obtained results confirm once again the dominant role of heat source in micro-hardness formation of the W9Mo4Co8 HSCP surface.

### 3.3 Results of Experimental Data Interpretation by Statistical Methods

Table 2 shows the results of the interpretation of Eq. (2) using statistical methods. The distribution curves of Eq. (2) are characterized by the kurtosis. From the standpoint of HSCP wear it is desirable that the skewness is negative:  $\tilde{y}_i > y_{i.}$ . In our study, such distributions of the experimental measures of position were 50%. This is evidenced by Eq. (2), the values of which were greater than one in that case. Final decisions were made on the expected reference values, for which the number of inequalities  $m\hat{y}_i > \hat{y}_{i.}$  increased to 9. The distinction between parametric and nonparametric reference values did not exceed 1-3%.

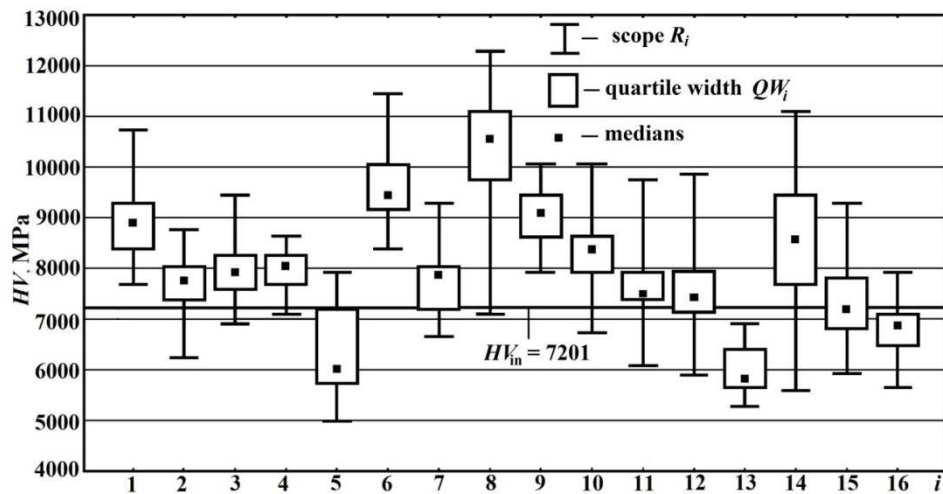


**Figure 2** Descriptive nonparametric statistics of the micro-hardness of the W9Mo4Co8 HSCP during grinding by wheels  $i = \overline{1;16}$ .

Part of the obtained information clearly illustrates the nonparametric descriptive statistics in Figure 2, squares represent experimental medians  $\tilde{y}_i$ ; rectangles represent quartile widths  $QW_i$ , covering 50% of the observations in Eq. (2); mustaches represent scopes  $R_i$ . Stationing of  $(\tilde{y}, R, QW)_i, i = \overline{1;16}$  in the same illustration gives a visual presentation of the distribution kurtoses of Eq. (2), their sign and location for 50% of the observations relative to the median. In this respect, the most favorable situation for strengthening an HSCP while grinding was formed by the wheels  $i = 1; 6; 9$  after all ground parts were obtained. Wheel 5A46 ( $i = 13$ ) had the worst cutting ability. Hence, all parts are characterized by softening during grinding. Wheels  $i = 8; 10; 14$  had more than 50% strengthening of their parts and can be recommended for grinding W9Mo4Co8 and W12V3Co10Mo3 HSCPs.

As can be seen from Table 2, there is a difference between the coefficients Eqs. (4) and (5) of the CA for wheels  $i = \overline{2;16}$  rating relative to the base tool *Norton Vitrium* ( $i = 1$ ). This demonstrates the feasibility of the second UVA stage with the search of expected reference values. The coefficients in Eq. (5) enhance the management capabilities of the grinding process with robust design operations using a multifactorial variance analysis model, constructed as basic tool.

**Table 3** Evaluation of wheel cutting ability by measure of micro-hardness dispersion Eqs. (6)-(8).

Wheels <i>i</i> = 1;16	$SD_i$	$R_i$	$QW_i$	$K_{Stij}$		
	$HV_i, \text{MPa/ B}_i, \%$			$j = 1(6)$	$j = 2(7)$	$j = 3(8)$
1	<u>685.978</u>	<u>3042.150</u>	<u>882.675</u>	<u>1.000</u>	<u>1.000</u>	<u>1.000</u>
	6.342	15.615	11.446	1.000	1.000	1.000
2	<u>660.712</u>	<u>2528.750</u>	<u>615.906</u>	<u>1.038</u>	<u>1.203</u>	<u>1.433</u>
	<u>553.267</u>	<u>2537.600</u>	<u>620.625</u>	<u>1.240</u>	<u>1.199</u>	<u>1.422</u>
3	4.260	12.070	5.736	1.486	1.294	1.995
4	<u>403.399</u>	<u>1542.350</u>	<u>486.094</u>	<u>1.700</u>	<u>1.972</u>	<u>1.816</u>
5	<u>834.521</u>	<u>2935.850</u>	<u>1424.519</u>	<u>0.822</u>	<u>1.036</u>	<u>0.620</u>
	<u>796.234</u>	<u>3070.700</u>	<u>896.800</u>	<u>0.862</u>	<u>0.991</u>	<u>0.984</u>
6	5.310	17.784	5.608	1.194	0.878	2.041
7	<u>646.712</u>	<u>2645.875</u>	<u>817.969</u>	<u>1.061</u>	<u>1.150</u>	<u>1.079</u>
	<u>1031.651</u>	<u>5203.600</u>	<u>1294.394</u>	<u>0.665</u>	<u>0.585</u>	<u>0.682</u>
8	6.233	20.114	6.950	1.018	0.776	1.647
	<u>558.167</u>	<u>2136.250</u>	<u>811.400</u>	<u>1.229</u>	<u>1.424</u>	<u>1.088</u>
9	3.766	13.349	6.950	1.684	1.170	3.465
10	<u>640.181</u>	<u>3321.450</u>	<u>714.850</u>	<u>1.072</u>	<u>0.916</u>	<u>1.235</u>
11	<u>722.777</u>	<u>3669.550</u>	<u>501.531</u>	<u>0.949</u>	<u>0.829</u>	<u>1.760</u>
12	<u>805.479</u>	<u>3964.300</u>	<u>776.813</u>	<u>0.852</u>	<u>0.767</u>	<u>1.136</u>
13	<u>486.204</u>	<u>1631.400</u>	<u>734.350</u>	<u>1.411</u>	<u>1.865</u>	<u>1.202</u>
14	<u>1341.464</u>	<u>5498.900</u>	<u>1654.706</u>	<u>0.511</u>	<u>0.553</u>	<u>0.533</u>
15	<u>787.930</u>	<u>3366.900</u>	<u>933.575</u>	<u>0.871</u>	<u>0.904</u>	<u>0.945</u>
16	<u>488.784</u>	<u>2261.550</u>	<u>596.744</u>	<u>1.403</u>	<u>1.345</u>	<u>1.479</u>

Note: Wheels *i* – see methodology of the experiment

### 3.4 Evaluation of Wheel Cutting Ability on the Basis of Dispersion Measures

The evaluation of wheel CA would be incomplete if the stability of their work is not taken into account. The measures of dispersion are presented in Table 3 and Figure 2. In the context of using nonparametric statistics, the emphasis was placed on quartile width. The measures of parametric method dispersion are given as ancillary ones. Additionally, it is advisable to involve descriptive nonparametric statistics in the discussion of the reproducibility of the grinding process (Figure 2) because the percentile  $(y_{0.75} - y_{0.25})_i$  may be located asymmetrically relative to  $\tilde{y}_i$  mentioned above.

Table 3 and Figure 2 demonstrate that wheels  $i = 4; 11$  showed the most stable performance for  $QW_i$  and the smallest precision was demonstrated by wheels  $i = 14; 8$ . Parametric methods for  $(R, SD)_i$  confirmed the highest stability of the

grinding process for wheel  $i = 4$ , and monocorundum wheel  $i = 13$  in the 2<sup>nd</sup> position.

Evaluation methods of both statistics coincide for the wheels that provide the highest precision of grinding. In practical terms,  $y_{0.25}$   $i = 8$ ; 14 are shifted above percentile  $y_{0.75}$  for most wheels that provide greater micro-hardness of the HSCP surface for details of the operating batch. This mainly concerns HPW  $i = 8$ .

#### 4 Conclusions

Instability of the grinding process determines the feasibility of nonparametric statistics application, which showed greater reliability of hypotheses adoption in terms of disarrangements of homoscedasticity and normality of the distributions. Under conditions of priority use of the nonparametric method as a parameter of wheel operational (work) stability, the quartile ranges should be used, which are still not widely spread in engineering practice.

Selected grinding mode:  $v_w = 35$  m/s;  $s_c = 1$  mm/double stroke;  $s_l = 7$  m/min;  $t = 0.015$  mm;  $z = 0.15$  mm, is characterized by increased depth of cut. This has made it possible to reveal the potential of the tested tools more adequately. It was found that the grinding of an HSCP made of W9Mo4Co8 steel by wheels 5NQ46I6VS3 ( $i = 1$ ), 5SG46K12VXP ( $i = 2$ ), 5SG60K12VXP ( $i = 3$ ), 5SG46I12VXP ( $i = 4$ ), 25AF46M12V5-PO ( $i=6$ ), 25AF46M12V5-PO3 ( $i=7$ ), 25AF46M10V5-PO ( $i = 8$ ), 25AF46M10V5-PO3 ( $i = 9$ ), 25AF46K10V5-PO3 ( $i = 10$ ), 25AF60M10V5-PO3 ( $i = 11$ ), 25AF46L10V5-KF35 ( $i = 12$ ), EKE46K3V ( $i = 14$ ), 92A/25AF46L6V20 ( $i = 16$ ) occurred without surface softening. In all other cases, the cutting temperature increase was accompanied by softening of the working surfaces of the HSCPs.

Precision estimations of wheel CA did not coincide with the results for the reference values. In particular, the greatest expected measures of position on the  $HV$  were predicted for 25AF46M10V5-PO ( $i = 8$ ), 25AF46M12V5-PO ( $i = 6$ ) and 25AF46M10V5-PO3 ( $i = 9$ ), which are presented in the form of a decreasing sequence. At the same time, the wheels 5SG46I12VXP ( $i = 4$ ), 25AF60M10V5-PO3 ( $i = 11$ ), 92A/25AF46L6V20 ( $i = 16$ ), 5SG46K12VXP ( $i = 2$ ) and 5SG60K12VXP ( $i = 3$ ) showed the greatest stability of the process.

Taking into account a comprehensive assessment of micro-hardness formation on the W9Mo4Co8 HSCPs by measures of position and dispersion, it is recommended to use wheels 5NQ46I6VS3 ( $i = 1$ ), 5SG60K12VXP ( $i = 3$ ),

5SG46I12VXP ( $i = 4$ ), 25AF46M10V5-PO3 ( $i = 9$ ), 25AF46K10V5-PO3 ( $i = 10$ ).

## References

- [1] Malkin, S. & Guo, Ch., *Grinding Technology: Theory and Applications of Machining with Abrasives*, 2<sup>nd</sup> ed., New York, Industrial Press, 375 pp., 2008.
- [2] Soler, Y. I. & Nguyen, V.C., *Microhardness of High-Speed P12Φ3K10M4 Steel Plates in Pendulum Grinding by The Periphery of Abrasive Wheels*, Russian Engineering Research, **35**(10), pp. 785-791, 2015.
- [3] Rudometov, Y.I., *Abrasive Tools Steeped in Special Suspensions*, Russian Engineering Research, **33**(6), pp. 381-383, 2013.
- [4] Rowe, W.B., *Principles of Modern Grinding Technology*, New York, William Andrew, 300 pp., 2009.
- [5] Geller, Y.M., *Tool Steels*, Moscow, Metallurgy Publ., 527 pp., 1983.
- [6] Kremnev, L.S., *Alloying Theory and Its Use for Creation of heat-Resistant Tool Steels and Alloys*, Metal Science and Heat Treatment, **50**(11–12), pp. 526-534, 2008.
- [7] Jackson, M.J. & Davim, J.P., *Machining with Abrasives*, New York, Springer, 429 pp., 2011.
- [8] Webster, J., & Tricard, M., *Innovations in Abrasive Products for Precision Grinding*, CIRP Annals – Manufacturing Technology, **53**(2), pp. 597-617, 2004.
- [9] Norton Saint-Gobain, *Abrasive Technological Excellence*, 2012.
- [10] Orhac, X., Jeevananthan, M., Krause, R. & Wu, M., Patent WO2007040865A1 PCT/US2006/033438, *Abrasive Tools Having a Permeable Structure*, Pub. 12.04.2007.
- [11] Soler, Y.I., Shustov, A.I. & Nguyen, M.T., *The Selection of High-Porous Boron Nitride Wheels Based on Topography of W9Mo4Co8 Plates for Pendulum Grinding using Fuzzy Logic*, Proceedings of Higher Educational Institutions, Machine Building, **7** (767), pp. 82-93, 2016.
- [12] State Standard GOST 9450–76, *Measurement of Microhardness Indentation of Diamond Tips*, Moscow, Standartinform Publ., 36 p, 1993.
- [13] Hollander, M., Wolfe, D.A. & Chicken, E., *Nonparametric Statistical Methods*, 3<sup>rd</sup> ed., New York, John Wiley & Sons, 844 pp., 2014.
- [14] Sachs, L., *Applied Statistics: A Handbook of Techniques*, 2<sup>nd</sup> ed., New York, Springer-Verlag, 707 pp., 1984.
- [15] State Standard GOST R ISO 5725–2–2002, *Accuracy (Trueness and Precision) of Measurement Methods and Results. Part 2: Basic Method for The Determination of Repeatability and Reproducibility of a Standard Measurement Method*, Moscow, Standartinform Publ., 62 pp., 2002.

- [16] Wheeler, D.J. & Chambers, D.S., *Understanding Statistical Process Control*, 3<sup>rd</sup> ed., Knoxville, SPC Press, 482 pp., 2010.
- [17] Soler, Y.I. & Nguyen, V.C., *Technological Reserves of Improving Grinding Quality of High-Speed Steel Plates with Improved Productivity*, Proceedings of Higher Educational Institutions, Machine Building, **5**, pp. 59-73, 2016.
- [18] Soler, Y.I., Kazimirov, D.Y. & Nguyen, V.L., *Quantitative Assessment of Burns While Flat Grinding Hardened Parts Made of Steel 37Cr4 by Abrasive Wheels of Different Porosity*, Metalworking, **1(66)**, pp. 6-19, 2015.
- [19] Starkov, V.K., *Grinding by High-Porous Wheels*, Moscow, Mechanical Engineering Publ., 688 pp., 2007.
- [20] Zubarev, Y.M. & Priemyshev, A.V., *Theory and Practice of Increasing The Efficiency of The Grinding of Materials*. Saint Petersburg, Lan' Publ., 304 pp., 2010.